Int J Adv Manuf Technol (2013) 65:1769–1778
DOI 10.1007/s00170-012-4298-6

ORIGINAL ARTICLE

On the role of form defects in assemblies subject to local deformations and mechanical loads

J. Grandjean · Y. Ledoux · S. Samper

Received: 6 March 2012 / Accepted: 7 June 2012 / Published online: 27 June 2012

Abstract Tolerancing activity is usually based on the traditional assumptions that surfaces have no form defects and are rigid under external loads. These assumptions tend to simplify the tolerance analysis of mechanical assemblies and hence the allocation of geometrical specifications. The present paper proposes an original procedure to systematically analyze and quantify the assembly of parts with form and position defects and deformable contact surfaces. Based on this procedure, stochastic simulations are performed by modifying the ratio between the position defects and form defects of surfaces. Even if the form defects are limited, they can lead to a non-compliant assembly. Clearly, the engineer's traditional approach, where form defects are assumed to have no influence, is generally not appropriate if we are to ensure that the expected performance is to be achieved on assembly.

Keywords 3D assembly · Form errors · Modal analysis · Positioning force · Local surface deformations · Noncompliance rate

1 Introduction

The continuous research into products that perform better, more energy-efficient, and more cost-effective has given rise to an increasing need to understand the influence of geometrical defects of parts, to develop means to measure these geometrical defects and to define a particular language with which to describe them. Faced with these challenges, geometric tolerances have been gradually introduced with the aim of providing a more comprehensive way to define allowable geometrical product variations subject to functional and technical requirements. Based on geometric tolerances, the designer transfers the functional requirements of the product onto functional specifications related to the different surfaces of the parts. These specifications define the extreme variations associated to shape, position, and orientation of geometrical features in order to guarantee the proper functioning of the final product.

Even if geometrical specifications are widely regarded as a key element to ensure a suitable level of quality for features, products, or assemblies, some restrictions still remain, based on intrinsic assumptions. In most cases, tolerance analysis quantifies and verifies the type and value of every geometrical specification, and for this, parts are supposed to be infinitely rigid and form defects are not considered.

It is not easy to integrate these two points since deformations in a part subject to loads (internal or external) usually require numerical processing (e.g., finite element simulations). In addition, the influence of the form error has to be based on a definition of defect types that are to be considered. Next, a particular procedure has to be developed to realize the assembly operation virtually and quantify defect influences in the tolerance analysis.

For answers to this question, we must understand the role of surface form defects when modifying the position of the part and integrate particular and more complex strategies into traditional tolerance analysis. By not considering form error in tolerance analysis, misevaluations can occur with

J. Grandjean · S. Samper
SYMME, Polytech 'Savoie,
BP 80439, 74944 Annecy-le-Vieux Cedex, France

Y. Ledoux (✉)
Univ. Bordeaux,
I2M, UMR 5295, Esplanade des Arts et Metiers,
F-33400 Talence, France
e-mail: yann.ledoux@u-bordeaux1.fr

regards to product performances, as has been shown recently by Grandjean [1]. These authors argue that even if the position tolerance is greater than twice the form error, some non-compliant assemblies could still be observed even when all geometrical specifications (form and position) have been respected. More to the point, the introduction of form defects may imply a large local contact pressure leading to local surface deformations. This concern represents another scientific bottleneck since introducing such mechanical joint behavior brings several nonlinearities into the resolution of the problem and consequently increases processing time.

To tackle such problems, the most common approaches developed in the literature rely on finite element simulations. To cite just a few studies, Jack et al. have developed the modeling and control of compliant assembly systems during the assembly process of a hood bracket. Chang, in [2], based on the stiffness matrix, simulated assembly and measurement processes to quantify the final geometrical assembly variations in the same way with the works of Cid [3], Hu [4], Stewart [5], and Söderberg [6]. Xie et al., in [7] examined the case of assembly and welding operations of stamping parts to consider both the positioning locators and clamping forces which deform the part. Interaction with the assembly is simulated by FEM through contact conditions. Pierre et al. have integrated thermo-mechanical deformations of compliant parts of a turboshaft engine [8]. All these papers deal with part deformations and propose methods to integrate these deviations into the tolerance analysis process.

Although scientific studies have made a great deal of progress in integrating such part deformations into tolerance analysis, the local deformations of functional contact surfaces are not addressed. This field has been intensively developed in tribology studies, where the behavior of contact surfaces is related to local pressure and associated deformations. A literature review by Bhushan in [9] and in Yu [10] showed that authors summarize several contact surface behaviors through numerical and analytical procedures. The main advantages of these models lie in the fact that they are tractable according to the required time to estimate local deformations due to external loads. More recent work dealing with local form defects and tolerance analysis has been addressed by Samper in [11] where an original concept of surface–sum defects is developed and used to simplify the consideration of surfaces with form defects. Finally, in preliminary studies by Le [12] on a simple planar joint, the influence of form defects is determined experimentally both from measurements of surfaces in contact and the relative mobility between one part and another.

Based on this review, the integration of both local deformations of functional surfaces and form defects represents a real scientific challenge concerning the development of a particular framework to enable them to be considered in the tolerance analysis process. It is also crucial to propose tractable processing compatible with the time available for the design process. These are the two main points covered in the present paper.

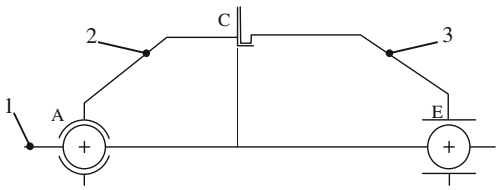

Fig. 1 Simplified representation of the mechanism

To illustrate our approach and the tools used, we have chosen a traditional assembly composed of two housings linked through a ball and cylinder joint added to a planar joint. This is the type of assembly usually used for pump bodies or turboshaft engine crankcases, as shown in Fig. 1. The main functional requirement is to position part 2 precisely in relation to part 3. These two parts position point A and point E respectively, ensuring the placing of the rotor in the crankcases. To achieve this functional requirement, the designer has to translate these requirements into geometrical specifications on the different features of the parts that make up the assembly (Fig. 2). In this figure, we propose to focus on a particular feature of part 2 located in joint C.

First, based on the technical drawings of this part, all extreme configurations of this feature are developed respecting the geometrical specification. This is the traditional three-dimensional calculation based on the worst case hypothesis. For this calculation, it is assumed that there are no form errors on parts. The result of this analysis is plotted on a particular graph representing the deviation domain. This point is detailed in Section 2. In Section 3, form errors are introduced. A case like this requires the generation of a particular base of defects, defined by a modal decomposition of the initial surface. Then, according to stochastic simulations, defect configurations are randomly composed to build a set of parts to be tested.

Next, a procedure has to be established for assembling parts by considering both (a) rigid parts with form and position defects, and (a) local deformations of parts with form and position defects subject to external loads. To have

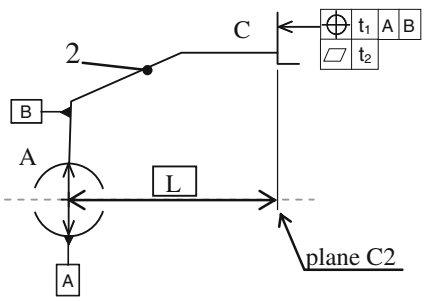

Fig. 2 Detail of the geometrical specifications of part 2

a general quantification of the influence of each of the phenomena, we propose to use the noncompliance rate.

2 Functional requirements

The goal of the tolerance analysis procedure is to verify the compliance of parts compared to the technical drawing. To achieve this, the concept of the deviation domain is used to determine the extreme displacement positions of joints corresponding to the boundary of the feasibility space, as first introduced by [13] and completed by Giordano by integrating the gaps between parts of a joint (also called clearance space) in [14, 15]. This concept is based on traditional assumptions where parts have no form defects and there is non-interference between parts. From the geometrical specification of location imposed by the designer, it is possible to determine all possible positions for plane C2. The representation and the associated processing are derived from previous studies (for more details, see [16–19]).

Consider point P_i on planar surface C2. In order to respect the location specification, all P_i points must remain within two parallel planes. The distance between these two planes corresponds to the tolerance value t. They are positioned on either side of the nominal plane (Fig. 3). In our study, the value of t corresponds to 50 μm and the inner and outer radii of the crankcase are r_i=90 mm and r_e=120 mm.

It is possible to determine all allowed displacements of P_i, noted $\delta\mathbf{p_i}$, corresponding to the small displacement of P_i. The relation is then written in Eq. 1.

$$\delta\mathbf{p_i}.\mathbf{z} \leq t_1 \tag{1}$$

The P_i Cartesian coordinates are defined in Eq. 2 as a function of nominal radius r of part 2, so that $\in[r_i, r_e]$ and $\theta \in[0, 2\pi]$.

$$P_i = (\cos(\theta).r, \sin(\theta).r, \Delta) \tag{2}$$

Thus, all allowed displacements of P_i, written in point O, are determined according to Eq. 3 where $\boldsymbol{\rho}$ corresponds to rotations of C2 planar surface along r_x and r_y axes and $\delta\mathbf{o}$ is the translation component (t_z axis) of the small (joint) displacements of C2 composed of three components (r_x, r_y, t_z).

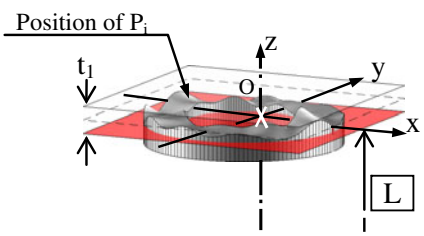

Fig. 3 Representation of the geometrical specification of the C2 annular flat surface

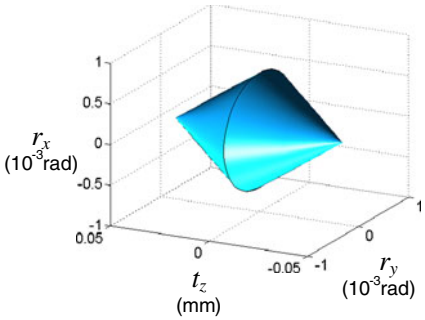

Fig. 4 Representation of all possible displacements of surface C2 according to the geometrical specification

The other three components are the kinematics components of the planar joint (t_x, t_y, r_z).

$$\delta\mathbf{p_i} = \delta\mathbf{o} + \mathbf{op_i} \times \boldsymbol{\rho} \tag{3}$$

Displacement $\delta\mathbf{p_i}$ along the z-axis can be explained by Relation 4.

$$\delta\mathbf{p_i}.\mathbf{z} = t_z + \cos(\theta).r.r_y - \sin(\theta).r.r_x \tag{4}$$

And according to Relation 1, the geometrical specification can be expressed by Relation 5.

$$-t_1/2 \leq t_z + \cos(\theta).r.r_y - \sin(\theta).r.r_x \leq t_1/2 \tag{5}$$

Relation 5 corresponds to the equation of two conic domains (two inequalities of Eq. 5) as shown in Fig. 4. It determines all extreme possible values of every geometrical parameter r_x, r_y, and t_z corresponding to the small displacement of the surface C2.

Consequently, referring to Eq. 5, it can be observed that all parameters of the rotations (r_x and r_y) and the parameter of translation (t_z) are linked. The extreme value of one parameter can only be obtained when all the others are null. Table 1 lists their extreme variation ranges.

3 Introduction of surface defects

It is well known that the geometry of any product is characterized by variability induced by the manufacturing processes which in turn affects functional performances. The generated form surfaces can be ranked from the microscopic scale (roughness) to the scale of the surface itself (form and position error). Taking such defects into account is not the usual approach used in tolerancing calculation. The simplest

Table 1 Extreme allowed value for all geometrical parameters

Geometrical parameter	t_z	r_x	r_y
Min. allowed value	$-t_1/2$	-atan($t_1/2.r$)	-atan($t_1/2.r$)
Max. allowed value	$t_1/2$	atan($t_1/2.r$)	atan($t_1/2.r$)

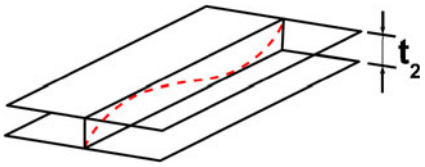

Fig. 5 Geometric parameters [38]

approach consists of characterizing deviation from the ideal surface (a plane in our case) by a unique scalar value t_2 representing the maximum amplitude of defects, as shown in Fig. 5 [20]. This is the method commonly used in the geometric tolerance approach. Another alternative would be to discretize the surface using a set of points (dotted line in Fig. 5), the parameters becoming their associated coordinates. This last approach leads to a very large number of parameters to manage.

Between these two extreme approaches, the literature proposes, for instance, polynomial models including Lagrangian interpolations, Bezier splines, and surfaces [21], which are often used in computer aided design. Such models are well suited to particular types of surface. A traditional method that can be applied whatever the surface consists of subdividing the initial feature into sub-surfaces. Another important class of methods based on periodic decomposition is also widely used. These methods could be based on Fourier series like the discrete cosine transform used for stamping processes [22], Zernike polynomials [23] used on disk-shaped surfaces in optics, or Fourier and Chebyshev polynomials used on cylindrical turned surfaces [24]. Modal discrete decomposition (MDD) is another way to model surface defects with few parameters. The major advantages of such an approach are the automatic build of the defect basis derived from natural eigenmodes of nominal surface and then allowing the automaticity of the procedure and the natural sorting of shape complexity. This last approach has been chosen in the present work to generate surface defects.

3.1 Modal discrete decomposition

Modal discrete decomposition is based on the computation of the natural modes of vibrations of surfaces. In our case, we have chosen to use the same feature (annulus) as the studied element. Thus, the annular surface is generated with a radius ranging from 90 to 120 mm. It is then discretized with 9,800 shell elements composed of four nodes (with $N = N_r x N_\theta$, $N_r = 71$, $N_\theta = 140$). Elements with three degrees of freedom (two rotations and one translation) were chosen. Every coordinate of the nodes that define the mesh of the part is achieved into a coordinate matrix **C** with 9,800 lines and three columns (for x, y, and z coordinates).

Based on the definition of every eigenmode of this discretized feature, a specific geometry set is defined. Each is used as a parameter defining the surface [25, 26]. To generate form error and undulation using modal decomposition, the eigenmodes of the annular flat surface must be determined first. They are obtained based on the solution of the dynamic conservative equilibrium given by Eq. 6, where **M** and **K** are the mass and stiffness matrices and **u** is the displacement vector.

$$\mathbf{M} \cdot \frac{\partial^2 \mathbf{u}}{\partial t^2} + \mathbf{K} \cdot \mathbf{u} = 0 \tag{6}$$

The solution of Eq. 6 provides a linear system to which the solutions are the eigenmodes $\boldsymbol{Q}_\mathbf{i}$ corresponding to the pulsation ω_i and **I** is the identity matrix.

$$\left(\mathbf{M}^{-1} \cdot \mathbf{K} - \frac{1}{\omega_i^2}\mathbf{I}\right) \cdot \boldsymbol{Q}_i = 0 \tag{7}$$

Solving Eq. 7, taking into account the free boundary conditions of the annular flat surface, gives:

1. The first three modes $\boldsymbol{Qr}_\mathbf{1}$ to $\boldsymbol{Qr}_\mathbf{3}$, corresponding to rigid body modes (rigid displacement of the surface)
2. The other modes $\boldsymbol{Q}_i$ (i=4,n), corresponding to the vibration modes of the surfaces

Each eigenvector is normalized according to the infinity norm so that $\|\boldsymbol{Q}_i\|_\infty = 1$. Basically, the amount of computed eigenmodes corresponds to the total number of degrees of freedom of the numerical models (in our case, 9,800). As an illustration, Fig. 6 represents the shapes of modes 4 to 9.

3.2 Generation of defect surfaces

From the analysis performed in Section 2, the extreme variation ranges of every geometrical parameter r_x, r_y and t_z are determined I, Table 1. The main concern in this section is to determine how the position defect and form defect are built. The procedure consists of adding a randomly selected configuration of position defects and then composing a form defect from the MDD basis. Each generated surface (i.e., with form and position/orientation defect) has to respect the geometrical specifications t_2 and t_1.

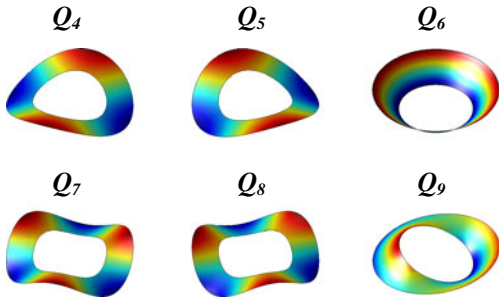

Fig. 6 Some natural modal surface shapes

Table 2 Definition of parameters related to uniform distribution of r_x, r_y and t_z

Parameter	t_{zr}	r_{xr}	r_{yr}
Associated distribution	$\boldsymbol{U}[-t_1/2;t_1/2]$	$\boldsymbol{U}[-\text{atan}(t_1/2r);\ \text{atan}(t_1/2r)]$	$\boldsymbol{U}[-\text{atan}(t_1/2r);\ \text{atan}(t_1/2r)]$

3.2.1 Position and orientation error

Let us consider three random parameters following continuous uniform probability density function (also called rectangular). Such a distribution has a constant probability function between its two parameters a (the minimum) and b (the maximum) and a random choice of configurations can be represented for the three position/orientation parameters. It is assumed that there are no dependencies between parameters. Knowing the extreme positions for each parameter (Table 1), three uniform distributions are then defined. Table 2 summarizes all the parameters and their associated distributions.

From these three distributions, several random choices of the triplet (t_{zr}, r_{xr}, and r_{yr}) are made. For each one, a test is performed to verify if the triplet remains inside the deviation domain (i.e., the tolerance location specification, see Eq. 4). If this triplet is valid, then these values are stored and are used to define the rigid transformation matrix, T, which characterizes the position and orientation error. It is used to position the nominal surface into a new surface called $\mathbf{C_p}$.

$$\mathbf{C_p} = T(\mathbf{C}) = \mathbf{C}.R + \boldsymbol{t}$$

where

$$R = \begin{bmatrix} 1 & 0 & 0 \\ 0 & c_x & -s_x \\ 0 & s_x & c_x \end{bmatrix} \begin{bmatrix} c_y & 0 & s_y \\ 0 & 1 & 0 \\ -s_y & 0 & c_y \end{bmatrix}; \quad (8)$$

$$c_x = \cos(r_{xr}); s_x = \sin(r_{xr}); c_y = \cos(r_{yr});$$

$$s_y = \sin(r_{yr}); \boldsymbol{t} = [0, 0, t_{zr}].$$

3.2.2 Form error

The definition of the form defect is based on the use of the eigenmodes previously computed. Since the position is defined independently of MDD, the first three MDD modes (corresponding to the rigid modes) are not considered. The procedure consists of combining every mode by a weight vector $\boldsymbol{w}$. All w_i follows a unitized and uniform distribution. Moreover, it was decided to scale every value of $\boldsymbol{w}$ as a function of the number of modes by a hyperbolic function. Such an approach was developed and justified in previous studies by Favrelière [27] and is highly suitable in cases where there is a turning part without an additional operation (e.g., grinding operation).

The $\mathbf{C_f}$ matrix is then calculated by combining all weighted modes from 4 to 400 according to Eq. 9. Figure 7 illustrates the procedure to generate surface defects. Surface $\mathbf{C_f}$ is built to respect the form tolerance specification t_2.

$$\mathbf{C_f} = \mathbf{C} \text{ and } \mathbf{C_f}.\mathbf{z} = \mathbf{C_f}.\mathbf{z} + \mathbf{Q}.\mathbf{w} \quad (9)$$

where $\mathbf{Q}$ is an N×n matrix of eigenmodes $\boldsymbol{Q_i}$, $\mathbf{z}$=[0, 0, 1] is the unit vector of the z-axis; $\mathbf{w}$=[w_1, w_2, … w_n] is a line vector of weight values.

Finally, the tested surface, $\mathbf{C'}$, is built from the surface with position/orientation defects ($\mathbf{C_p}$) added to the surface with form defects ($\mathbf{C_f}$), as proposed in Eq. 10. A schematic representation of this addition is plotted in Fig. 8.

$$\mathbf{C}' = \left[\mathbf{C_p}.\mathbf{x} \quad \mathbf{C_p}.\mathbf{y} \quad \left(\mathbf{C_p}.\mathbf{z} + \mathbf{C_f}.\mathbf{z}\right)\right] \quad \text{With } \mathbf{x} = [1, 0, 0] \text{ and } \mathbf{y} = [0, 1, 0]; \quad (10)$$

The final surface $\mathbf{C'}$ is assumed to be compliant only if the extreme amplitude along the z-axis remains below the tolerance specification t_1. It can be calculated according to these two inequalities written in 11.

$$\max(\mathbf{C}'.\mathbf{z})t_1/2 \text{ and } \min\ (\mathbf{C}'.\mathbf{z}) - t_1/2 \quad (11)$$

The same procedure is followed for both surfaces, C2 and C3 (where surface C belongs to parts 2 and 3 of the assembly, as shown in Fig. 1).

4 Simulation of assembly phase

The previous section described the generation of surfaces with position/orientation and form defects. A procedure to perform the assembly of such surfaces is required and will be applied to planar surfaces C2 and C3. Since the real assembly of these two surfaces is performed by a set of screws and nuts, it is assumed that it will be modeled by a vertical load along the z-axis. This external load is named $\mathbf{F_{ext}}$ in the following.

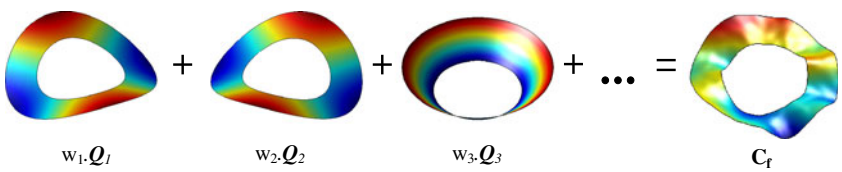

Fig. 7 Generation of the surface defect

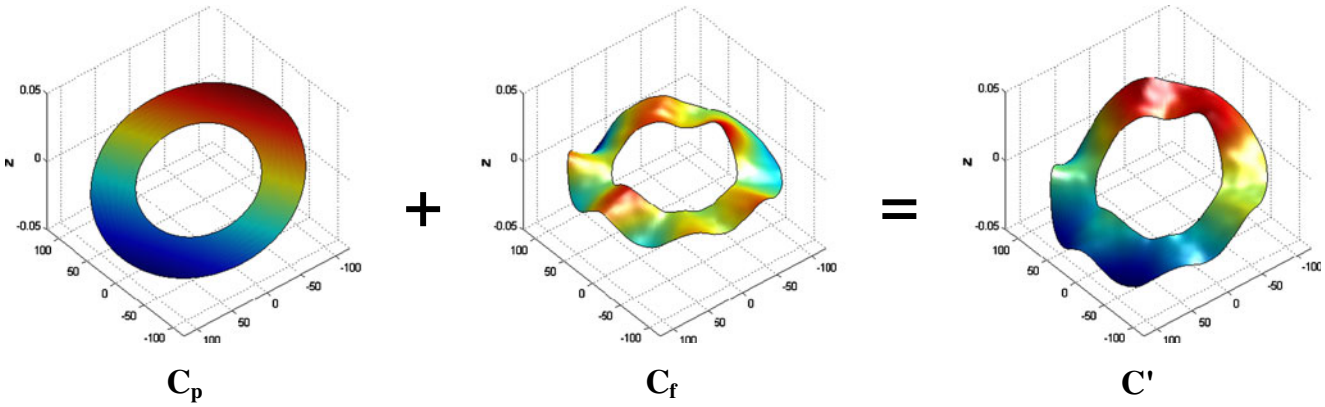

Fig. 8 Schematic addition operation of position and form defects

To simplify this numerical assembly phase, we use the artifact of the surface–sum concept introduced by [25, 28]. It consists of transferring all part defects into only one part, the other one being perfectly flat. Deviations can be taken into account using a stack up assembly method [29]. Since the surface–sum concept corresponds to the addition of the defects in the two parts, 2 and 3, the allowable tolerance zone of the surface–sum must be redefined. It becomes the sum of each tolerance of the initial surface C2 of parts 2 and 3. Thus, the tolerances can be calculated according to Eq. 12.

$$\begin{aligned} t_{f1} &= t_{1(\text{part2})} + t_{1(\text{part3})} \\ t_{f2} &= t_{2(\text{part2})} + t_{2(\text{part3})} \end{aligned} \tag{12}$$

In the case studied here, both tolerance $t_{1(\text{part 2})}$ and $t_{1(\text{part 3})}$ are the same and are equal to 50 μm. The final value of t_{f1} corresponds to 0.1 mm. A similar procedure is performed to determine the form tolerance t_{f2}.

4.1 Assembly procedure with rigid surfaces

In this step, it is assumed that all surfaces are rigid. For each generated surface, the associated surface–sum is deduced. The procedure then consists of identifying the matting facet that makes up the three contact points positioning the part. To assure the mechanical equilibrium of the part subject to load $\mathbf{F_{ext}}$, the matting facet has to be intersected by the matting force. Figure 9 illustrates the main phases of the procedure. The different components of position can be deduced composed of t_z, r_x, and r_y.

4.2 Assembly procedure with local surface deformations

Considering local deformations in the case of contact surface with form defects is not an easy task as argued in the literature by [30, 31], either in terms of theoretical or numerical implementation. In the example studied here, consisting of two nominal flat surfaces placed in contact, form defects (i.e., roughness and undulation) cause contacts at discrete contact spots (Fig. 10). A stress state arises from local deformations of these local contacts that are opposed to the external load $\mathbf{F_{ext}}$ (pressing one surface of the carter onto the other). The load value, $\mathbf{F_{ext}}$, corresponds to 1,100 N. The sum of these contact spots constitutes the real area of contact and corresponds, most of the time, to a fraction of the nominal surface that makes up the mechanical joint. In the literature, several mechanical models have been developed based on analytical relations. Articles [9, 32] provide a general overview of different models.

In our preliminary work, local deformations and associated stresses are modeled by a purely plastic behavior of the

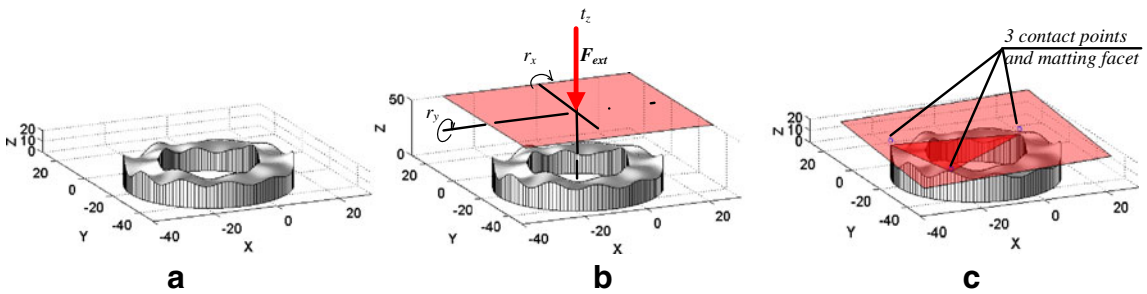

Fig. 9 Diagram showing the different phases in defining the matting face; **a**. Initial surface–sum with form and position defects; **b**. Determining the direction of the external load Fext and the position parameters; **c**. Defining the position (r_x, r_y, and t_z) as a function of the matting facet

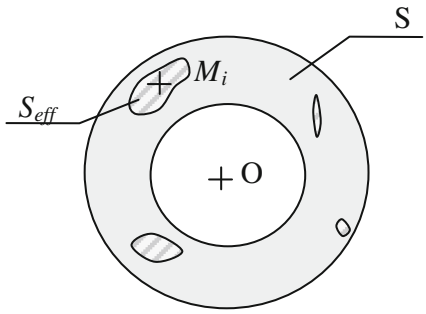

Fig. 10 Illustration of the different zones of effective contact surface (S_{eff}) and definition of position O, center of the part, and point M_i included in the contact surface

material (also called erosion model). In such a case, the value of the real contact pressure is bounded by the hardness H of the material, which can be approximated by 2.8 times the yield stress (according to [33]).

In general, the equilibrium of the plane surface with defects can be calculated by Eq. 13.

$$\begin{cases} \int_s \boldsymbol{f}(Mi).ds = \mathbf{F_{ext}} \\ \int_s \boldsymbol{f}(Mi) \times \mathbf{OM}_i.ds = \mathbf{0} \end{cases} \quad (13)$$

Where $\boldsymbol{f}(Mi)$ corresponds to the distribution function of the elementary forces located at point Mi; $\mathbf{F_{ext}}$ corresponds to the external mechanical load and × is the cross vector product operator.

According to the erosion procedure, the function $\boldsymbol{f}$ corresponds to a constant. Furthermore, by introducing the apparent contact pressure, called P, given by $P=\mathbf{F_{ext}}/S$, where S is the total area of the annular contact of inner and outer radii r_0 and r_1; $S=\pi(r_1^2-r_0^2)$, Eq. 13 can be simplified as in Eq. 14.

$$\begin{cases} P = H.\dfrac{S_{eff}}{S} \\ \int_s \boldsymbol{OM_i}.ds = 0 \ such\ as\ M_i \in S_{eff} and\ \boldsymbol{O}\ is\ \ the\ center\ \ of\ \ the\ part \end{cases} \quad (14)$$

where H corresponds to the hardness 1,800 MPa of the material, S_{eff} is the effective surface in contact.

By solving this system of equations, the position of the surface defect can be deduced as a function of two angular parameters along the x (r_x) and y axes (r_y) and a translation along the z-axis (t_z).

5 Results

The main focus of this applied section is to exploit the various procedures for generating and assembling different parts with different combinations of defects and then to draw conclusions on the influence of the surface defects in the final position of part 2 compared to part 3 of the crankcase. The comparison is based on the computation of the noncompliance rate of assembly according to stochastic simulation. To do this, sets of 10,000 parts with different profiles of defects were generated. To quantify the influence of the position defect compared to the form defects, we performed a parametric study where t_1 is fixed to 0.1 mm and t_2 ranges from 0 (no form defect) to 0.1 mm (the amplitude of form defect is equal to the position defect). Both kinds of assembly, with or without local deformations, were carried out. By using graphic representation, we were able to identify whether the assembly respects the function requirement. If the SDT component (respectively, r_x, r_y, and t_z values) remains inside the deviation domain identified in Section 2, the assembly is possible, otherwise, it is nonconform. These last non-conform assemblies are plotted in Fig. 11 by points surrounded by a blue circle.

Table 3 summarizes the main results of this parametric study. First, in the case of null form defect, it can be seen that all tested assemblies are compliant. This configuration follows the usual assumptions regarding tolerance analysis and enables us to validate the procedure (case of rigid assembly and no form defect). In this case, introduction of local deformation does not modify this noncompliance rate. This phenomenon corresponds to the optimal contact condition (the entire annular surface in contact). In such contact

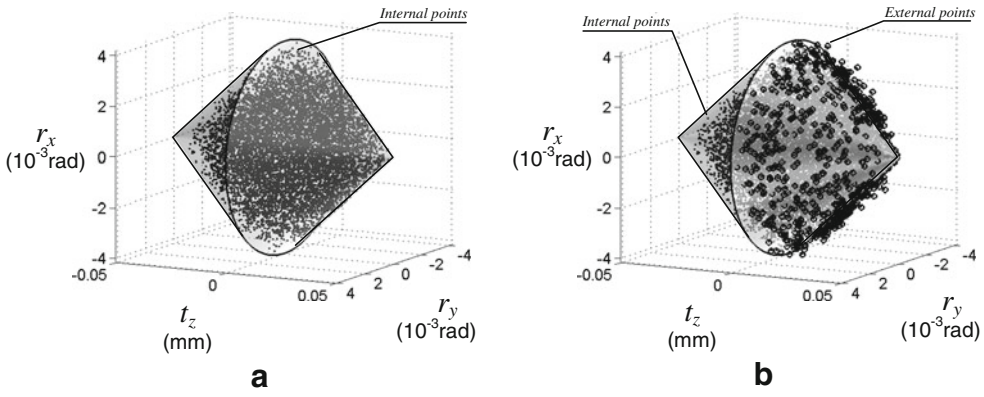

Fig. 11 Representation of two sets of 10,000 assemblies by considering rigid surface with: **a** t_1=0.1 mm and t_2=0 mm (no form defect); **b** t_1=0.1 mm and t_2=0.025 mm

Table 3 NCR of the assembly according to t_2 value

t_2 (t_1=0.1 mm)	0 mm	0.025 mm	0.05 mm	0.075 mm	0.1 mm
Non Compl. Rate with rigid model (%)	0	7.66	11.34	13.91	14.71
Non Compl. Rate with local def. (%)	0	6.42	8.99	10.92	11.08

conditions, based on the hardness of the surface, the induced displacement can be estimated to remain below 1/100 μm. It can be seen that the corresponding local displacement becomes negligible compared to the position defects.

In order to test surfaces with form defects, t_2 is increased. This leads to more non-conform assemblies. By keeping in mind that all tested surfaces are compliant when compared to the initial functional requirements, this trend shows the limit of the traditional tolerance specification approach. Figure 11 is a representative sample of all results obtained. In the case of no form defect, all points remain in the specification zone (bi-conical blue area). In addition to this point, the angular deviation of each assembly tends to increase due to the slope of the matting facet, which can move the initial position of the surface determined from the position/orientation components.

When local surface deformations (last line of the Table 3) are introduced, we observe a decrease in the noncompliance rate. This can be explained by the direction of the external load ($\mathbf{F_{ext}}$), centered along the z-axis of the crankcase, which compensates the initial deviation of the surfaces. Due to the form defects, the extreme asperities of contact are eroded and then the matting surface orientation is forced to reorient along the z-axis. Consequently, the rotation components and the translation along z are lowered. This phenomenon influences a small percentage of the NCR (noncompliance rate).

6 Discussion

In studying this example, we highlight the influence of form defects in the functional surfaces of a mechanical joint. Engineers have always defined the location tolerance for positioning the surface on the basis of functional requirements. More to the point, it is crucial to limit surface form defects by adding a flatness specification. Usually, the value of the locating tolerance is calculated according to the functional geometrical specification expected of the mechanism. The form specification is then deduced by using empirical rules. A position/form defect ratio of more than 2 is commonly used. In this study, with a simple assembly composed of two parts, it has been shown that a noncompliant assembly can be achieved even if this ratio remains relatively low (t_1/t_2=4, NCR=7 %).

To improve this ratio, it is necessary to select a more accurate means of production or to add finishing operations on machined surfaces, which would result in higher production costs. A compromise therefore has to be reached between the accuracy of the shape of the surface and the admissible level of noncompliance rate. The present work makes some contribution to quantifying the influence of the position/form defect ratio (t_1/t_2) on the noncompliance rate. Numerical processing is performed within a reasonable time. With the rigid assembly, only a few minutes are required to test 10,000 assemblies; processing is longer in the case of local deformation, and takes a few hours. This increase in the time required is mainly due to the nonlinearity of the problem when mechanical equilibrium is defined (angular position of surface).

We have also shown the influence of external loads on the mechanism, corresponding to the assembly phase of the crankcase (with nuts and screws). In the example, the load tends to bring the two surfaces together and thus reduce position error. To simulate this phenomenon, a simple model of local deformation has been developed assuming a purely local behavior on the part of plastic surfaces. Despite these simplifications, it is possible to identify the trends of the assembled surfaces subjected to loads and then to predict the behavior of the final assembly.

For deepening this concept of assembly with form and position defects and deformable contact parts of mechanisms, it would be interesting to carry out experimental trials to test and validate the results obtained in this study. This needs to manage the defect measurement of contact surfaces, the direction of the external mechanical loads, and then to isolate the different sources of deformation (housing/local contact). For that purpose, a particular experimental device is being designed and different experiments will be initiated to validate the relevance and the accuracy of the developed approach.

However, others authors like Ballu et al. [34] have already experimented this approach and underline the influence of form defects on surface assembly in case of planar contact surface. More to the point, the procedure and the various tools used in this paper have been validated through various studies. We can cite the work of Favreliere et al. [35] and Adragna et al. [36] for the characterizations of assembling sets with both form and position defects and, more recently, [37] for sealing joint.

Finally, the approach developed here is based mainly on particular surface defects chosen beforehand. The challenge is then to customize a particular base of defects according to the selected means of production. To do this, it is then necessary to define the main defects generated by that

means of production. It could then be possible to make a projection of these technological defects into the modal base. The defects that are the most penalizing on the accuracy of assembly could then be identified. It would also be possible to differentiate the different processes as function of the type of form defects generated.

7 Conclusion

To guarantee the proper functioning of a mechanical assembly, designers have to specify the expected geometrical accuracy of every functional surface of parts through geometrical constraints. Tolerancing corresponds to such an engineering activity and consists of analyzing and quantifying the influence on functional requirements of surface defects in size and position. Such studies have traditionally been based on assumptions that surfaces have no form defects and are supposed to be rigid. The present paper highlights the influence of surface defects regarding the functional specifications of a mechanism. For this, a systematic approach has been developed. First, a particular basis of form defects is computed from a decomposition of the surface according to natural vibrational eigenmodes. Next, surface defects are built from random composition defects in modal discrete decomposition. A particular assembly procedure is then developed, considering both the position and the form defects of surfaces. Two cases are envisaged: (a) surfaces with defects are assumed to be rigid; (b) surfaces with defects are assumed to have local deformations subject to external mechanical loads. Based on these two contact surface behaviors, the noncompliance rate of the assembly is quantified. When form defects are not considered in the tolerance analysis procedure, this leads to non-compliant manufacturing assembly, and this is one of the major conclusions of this work.

Although this is an original approach using simulations of assemblies with both surface defects and external mechanical loads for an acceptable processing duration, some limitations can be pointed out which will lead in turn to future improvements. First, the basis of defects was built without any consideration given to the process used (turning, milling) although it is well known that specific types of defects can depend on the process used (e.g., conicity defects, apparition of lobes in the plane surface due to concentric clamping jaws, etc.). This point can be solved by defining beforehand a basis of defects related to technological defects according to production means. This set of parameters will be called the technological form basis and will help engineers to identify and then control the production process (tool setting) according to defect type. The modal shape basis can be modified by adding those technical form shapes in order to build a new shape basis. We can also see if the technical shapes are well defined or not according, for instance, to parameter criticality.

Furthermore, in order to limit the complexity of integrating local surface deformations and as we were assuming small contact surfaces, it was decided to develop a purely plastic behavior in the contact model. By considering a more complex behavior, such as an elastoplastic model, this can improve the accuracy of the local deformations. The assembly procedure developed in this paper will remain identical, except for the time required, as the nonlinearities introduced by the mechanical models make the computation of the mechanical equilibrium procedure more complex.

Finally, in this study it was assumed that only the functional surfaces in contact, subject to the applied loads on the structure, are deformed. However, it would be more realistic in the case of thin parts to also consider global structure deformations that are added to the local surface deformations. These could lead to a more accurate behavior of the assembly both in static and in dynamic state (consider the evolution of the load as a function of time). To achieve this, it could be necessary to use finite element software, for example, to compute the structure deformations as has already been proposed in the literature (e.g., [6–8]). Another alternative is to characterize the stiffness matrices of structures around the functional surfaces and then integrate them into the tolerancing model.

Acknowledgments The authors acknowledge the financial support from the French Ministry of Research, the European Union, the "Assemblée des Pays de Savoie", the Competitiveness Pole "Arve Industrie Haute Savoie Mont-Blanc", and the Carnot MIB.

References

1. Grandjean J, Ledoux Y, Samper S (2011) Influence of form errors in plane surfaces assemblies, IMProVe, International Conference on Innovative Methods in Product Design, Venice, Italy, 15-17/6
2. Chang M and Gossard DC (1997) Modeling the assembly of compliant, non-ideal parts, computer-aided design. Vol. 29, No. 10, pp. 701–708
3. Cid G, Thiebaut F, Bourdet P, Falgarone H (2007) Geometrical study of assembly behaviour, taking into accounts rigid components' deviations, actual geometric variations and deformations, J.K. Davidson (Ed), Models for computer-aided tolerancing in design and manufacturing, 301 310 Springer
4. Jack Hu S, Camelio J (2006) Modeling and control of compliant assembly systems. CIRP Ann Manuf Technol 55(1):19–22
5. Stewart ML, Chase KW (2005) Variation simulation of textured assembly for compliant structures using piecewise-linear analysis. Am Soc Mech Eng 16–1:591–600
6. Söderberg R, Lindkvist L, Dahlström S (2006) Computer-aided robustness analysis for compliant assemblies. J Eng Des 17:411–428
7. Xie K, Wells L, Camelio JA, Youn BD (2007) Variation propagation analysis on compliant assemblies considering contact interaction. J Manuf Sci Eng Trans ASME 129(5):934–942

8. Pierre L, Teissandier D, Nadeau JP (2009) Integration of thermo-mechanical strains into tolerancing analysis. Int J Interact Des Manuf 3:247–263
9. Bhushan B (1998) Contact mechanics of rough surfaces in tribology: multiple asperity Contact. Tribol Lett 4:1–35
10. Yu MM-H, Bhushan B (1996) Contact analysis of three-dimensional rough surfaces under frictionless and frictional contact. Wear 200(1–2):265–280
11. Samper S, Adragna PA, Favreliere H, Pillet M (2009) Modeling of 2D and 3D assemblies taking into account form errors of plane surfaces. J Comput Inf SciEng Vol. 9–4
12. Le H. N., Ledoux Y., Darnis P., Ballu A., Experimental comparison between displacements and surface defects measurements applied to planar joint, IMProVe, International Conference on Innovative Methods in Product Design, Venice, Italy, 15-17/6, 2011
13. Turner JU (1993) A feasibility space approach for automated tolerancing. J Eng Ind 115:341–346
14. Giordano M, Duret D, Tichadou S (1992) Clearance space in volumic dimensioning. Anal CIRP 41/1:565–568
15. Giordano M, Pairel E, Samper S (1999) Mathematical representation of tolerance zones, Proceedings of 6th CIRP seminar on computer-aided tolerancing, Kluwer, 177–186
16. Bourdet P, Ballot E (1995) Geometrical behavior laws for computer-aided tolerancing. Proceedings of 4th CIRP Seminar on Computer Aided Tolerancing (ed. F. Kimura), pp. 143–153
17. Clozel P (2001) 3D tolerances analysis from preliminary study, Proceedings of the 7th CIRP Seminar on Computer Aided Tolerancing (ed. P. Bourdet & L. Mathieu), pp. 93–104, Kluwer academic publisher
18. Clément A, Bourdet P (1988) A study of optimal-criteria identification based on the small-displacement screw model. Annals of the CIRP Vol. 37/1/1988, ISBN 1-40201423-6
19. Ballu A, Mathieu L (1999) Choice of functional specifications using graphs within the framework of education. Proceedings of 6th CIRP Seminar on Computer Aided Tolerancing ISBN 0-7923-5654-3, 197–206, Kluwer academic publisher
20. Mokhtarian F, Mackworth AK (1992) A theory of multiscale, curvature-based shape representation for planar curves. IEEE Trans Pattern Anal Mach Intell 14(8):789–805
21. Gupta S, Turner JU (1993) Variational solid modeling for tolerance analysis. IEEE Comput Graphics Appl 13(3):64–74
22. Huang W, Ceglarek D (2002) Mode-based decomposition of part form error by discrete-cosine-transform with implementation to assembly and stamping system with compliant parts. CIRP Ann 51:21–26
23. ISO 10110–5, Optics and optical instruments—preparation of drawings for optical elements and systems—Part 5: surface form tolerances, International Organization for Standardization, 1996
24. Henke RP, Summerhays KD, Baldwin JM, Cassou RM, Brown CW (1999) Methods for evaluation of systematic geometric deviations in machined parts and their relationships to process variables. Precis Eng 23:273–292
25. ISO 1101 (1983) Technical drawings—geometrical tolerancing—tolerancing of form, orientation, location and run-out—generalities, definitions, symbols, indications on drawings, International Organization for Standardization
26. Samper S, Formosa F (2007) Form defects tolerancing by natural modes analysis. J Comput Inf Sci Eng 7(1):44–51
27. Huang Q-X, Wicke M, Adams B and Guibas L (2009) Shape decomposition using modal analysis, 28(2), Eurographics, 30 March-3 April, Munich, Germany
28. Favreliere H (2009) Tolérancement modal, de la métrologie vers les spécifications, University of Savoie PhD thesis
29. Greenwood J, Williamson J (1966) Contact of nominally flat surfaces. Proc R Soc London Ser A 295(1442):300–319
30. Mathieu L, Villeneuve F (2010) Geometric tolerancing of products. ISTE Ltd and John Wiley & Sons Inc.
31. Hyun S, Pei L, Molinari JF, Robbins MO (2004) Finite-element analysis of contact between elastic self-affine surfaces. Phys Rev E
32. Pei L, Hyun S, Molinari JF, Robbins MO (2005) Finite-element modeling of elastoplastic contact between rough surfaces. J Mech Phys Solids
33. Kadin Y, Kligerman Y, Etsion I (2006) Unloading an elastic–plastic contact of rough surfaces. J Mech Phys Solid 54 (12):2652–2674
34. Tabor D (1951) The hardness of metals. Clarendon Press, Oxford, UK
35. Ballu A, Jay A, Darnis P (2010) Experimental evaluation of convex difference surface for planar joint study. Idmme-Virtual Concept, Bordeaux
36. Favreliere H, Samper S, Adragna P-A, Giordano M (2007) 3D statistical analysis and representation of form error by a modal approach, Computer Aided Tolerancing (CAT), Erlangen, Germany
37. Adragna P-A, Samper S, Pillet M, Favreliere H (2006) Analysis of shape deviations of measured geometries with a modal basis. J Mach Eng: Manuf Accuracy Increasing Problems, Optimization 6 (1):134–143
38. Ledoux Y, Lasseux D, Favreliere H, Samper S, Grandjean J (2011) On the dependence of static flat seal efficiency to surface defects. Int J Pres Ves Pip 88(11–12):518–529